

<sup>6</sup>Han, Y. M., and Hahn, H. T., "Ply Cracking and Property Degradation of Symmetric Balanced Laminates Under General In-Plane Loading," *Composites Science and Technology*, Vol. 35, No. 4, 1989, pp. 377–397.

<sup>7</sup>Bert, C. W., Reddy, J. N., Choa, W. C., and Reddy, V. S., "Vibration of Thick Rectangular Plates of Bimodulus Composite Material," *Journal of Applied Mechanics*, Vol. 48, No. 2, 1981, pp. 371–376.

<sup>8</sup>Rebello, C. A., Bert, C. W., and Gordaninejad, F., "Vibration of Bimodular Sandwich Beams with Thick Facings: A New Theory and Experimental Results," *Journal of Sound and Vibration*, Vol. 90, No. 3, 1983, pp. 381–397.

<sup>9</sup>Gordaninejad, F., "Bending of Thick Angle-Ply Bimodular Composite Plates," *AIAA Journal*, Vol. 28, No. 11, 1990, pp. 2005–2008.

<sup>10</sup>Shahid, I., and Chang, F.-K., "An Accumulative Damage Model for Tensile and Shear Failures of Laminated Composite Plates," *Journal of Composite Materials*, Vol. 29, No. 7, 1995, pp. 926–981.

<sup>11</sup>Erdman, D. L., and Weitsman, Y., "The Multi-Fracture Response of Cross-Ply Ceramic Composites," *International Journal of Solids and Structures*, Vol. 35, No. 36, 1998, pp. 5051–5083.

<sup>12</sup>Daniel, I. M., and Ishai, O., *Engineering Mechanics of Composite Materials*, Oxford Univ. Press, New York, 1994, p. 35.

A. N. Palazotto  
Associate Editor

## Probabilistic Finite Element Model Updating Using Random Variable Theory

Loukas Papadopoulos\* and Ephraim Garcia†  
Vanderbilt University, Nashville, Tennessee 37235

### Introduction

THE finite element (FE) method is a popular technique used to determine structural responses of complex structures. However, modal surveys performed on actual hardware do not always agree with analytically predicted natural frequencies and mode shapes. The goal of model updating/refinement, therefore, is to correct the deficiencies found within the analytical FE model. There are several classes of model updating schemes. The simplest ones are direct updating in which mass and/or stiffness matrices are updated in a single iteration, such as in Ref. 1. Another class of schemes utilize sensitivity methods.<sup>2</sup> A detailed overview/survey of model updating techniques in structural dynamics is provided by Imregun and Visser<sup>3</sup> and Mottershead and Friswell.<sup>4</sup>

In the past, dynamic systems have been assumed to have well-defined structural properties or to have small variations in them. A deterministic analysis is then usually performed to obtain the desired result, that is, static or dynamic analysis. However, systems may not always be well defined, and a stochastic analysis must be performed. Modal parameter uncertainty, for example, may arise from randomness in the structural properties (due to manufacturing variability), from measurement errors (e.g., noisy sensors), statistical variations in the measurement process (e.g., inaccurate data acquisition system), and/or variations with all of the myriad of system identification algorithms. Repeated experimentation will also exhibit modal parameter variations.

These modal parameter variations will be explored to improve the robustness characteristics of current model updating methodologies. As a result, all uncertainty will be quantified by treating the stiffness (or, in this case, flexural rigidity  $EI$ ) as random with an associated probability density function. Because of the mathematics involved, a

caveat that should be stated is that the number of experimental modes measured is required to be the same as the number of unknowns in the problem, thus allowing for a unique solution. Note that this assumption is very limiting when relating to any realistic problem, but the intent of the Note is to show the method. Finally, note that Papadopoulos and Garcia<sup>5</sup> applied this technique using noise-free simulated data on a cantilever Euler–Bernoulli beam and found that the method is able to correct the errors in the initial FE model. This Note adds to the previous work by evaluating the technique using actual experimental data from a similar cantilever beam. In addition, the underlying methodology for this technique is a modification of the damage detection theory formulated by Papadopoulos and Garcia.<sup>6,7</sup>

### Theoretical Development

The main development of this technique may be found in Ref. 5 and in related reference materials.<sup>6,7</sup> On considering the free vibration eigenvalue problem for an  $N$ th-order undamped dynamic system and assuming that the initial analytical uncorrected model is related to the experimental model by an amount  $\Delta$ , we arrive at the principle equation

$$\Delta \lambda_i \{\phi^a\}_i^T [M^a] \{\phi^{ex}\}_i = \sum_{j=1}^L \alpha_j \{\phi^a\}_i^T [K_j^e] \{\phi^{ex}\}_i \quad (1)$$

for  $i = 1, 2, 3, \dots, N$ , where quantities with a superscript  $a$  denote initial analytical data and  $ex$  denotes experimental data.  $[M^a]$  represents the  $(N \times N)$  symmetric analytical mass matrix,  $[K_j^e]$  denotes the sparse analytical  $j$ th element stiffness submatrix,  $\lambda_i$  is the  $i$ th mode scalar eigenvalue,  $\{\phi\}_i$  is the  $i$ th mode eigenvector or mode shape of size  $(N \times 1)$ , and  $\alpha_j$  represents the  $j$ th element stiffness reduction factor (SRF). The SRFs indicate the amount of stiffness correction required for each  $j$ th element to accommodate the non-agreement between the analytical and experimental modal parameters. For example, a value of  $-0.5$  indicates that the elemental stiffness needs to be reduced by 50%, and a value of  $+0.5$  indicates that it needs to be increased by 50%.  $L$  denotes the total number of structural elements comprising the system, and  $T$  denotes a matrix transpose.

Equation (1) represents a set of  $N$  simultaneous linear equations with  $L$  unknowns that can be written in the form of

$$[A]_{(N \times L)} \{q\}_{(L \times 1)} = \{b\}_{(N \times 1)} \quad (2)$$

whose elements are given as

$$\begin{aligned} A_{ij} &= \{\phi^a\}_i^T [K_j^e] \{\phi^{ex}\}_i \\ q_j &= \alpha_j \\ b_i &= \Delta \lambda_i \{\phi^a\}_i^T [M^a] \{\phi^{ex}\}_i \\ &= (\lambda_i^{ex} - \lambda_i^a) \{\phi^a\}_i^T [M^a] \{\phi^{ex}\}_i \end{aligned} \quad (3)$$

for  $i = 1, 2, \dots, N$  and  $j = 1, 2, \dots, L$ . The vector  $\{q\}$  in Eq. (2) represents the SRFs for each structural element. In general, the number of experimentally measured modes  $N$  will be less than the total number of individual structural elements  $L$  of the system. Therefore, the matrix  $[A]$  will be rectangular and noninvertible, that is, a set of underdetermined systems of equations. For the special case when  $N = L$ , there will be a unique solution because  $[A]$  will be square and invertible. This Note will focus on the ideal case when  $N = L$  (although this will not be the case for any realistic problems), thereby permitting a unique solution. Note that this assumption is very limiting when relating to any realistic problem, but the intent of the Note is to show the method. The quantities in Eq. (2) will be treated as random variables assumed to have normal distributions, where the expected value and covariance matrix of the unknowns  $\{q\}$  are found in Ref. 5.

### Results

To illustrate the proposed method, the theory will be applied to the model correction of an aluminum cantilever Euler–Bernoulli beam using experimental data. The beam used in the experimental

Received 22 March 1999; revision received 24 August 2000; accepted for publication 31 August 2000. Copyright © 2000 by the American Institute of Aeronautics and Astronautics, Inc. All rights reserved.

\*Graduate Research Assistant, Smart Structures Laboratory, Department of Mechanical Engineering.

†Professor, Center for Intelligent Mechatronics, Department of Mechanical Engineering; currently Program Manager, Defense Sciences Office, Defense Advanced Research Projects Agency, Arlington, VA (on leave from Vanderbilt University). Member AIAA.

Table 1 Mean SRFs from Eq. (2) and Monte Carlo simulation

Scheme	Mean beam superelement SRFs				
	$\alpha_1$	$\alpha_2$	$\alpha_3$	$\alpha_4$	$\alpha_5$
Case A					
Eq. (2)	0.0652	0.0386	0.0410	0.0525	0.0326
Monte Carlo simulation	0.0600	0.0557	0.0538	0.0604	0.0536
Case B					
Eq. (2)	-0.0362	-0.0603	-0.0581	-0.0478	-0.0657
Monte Carlo simulation	-0.0410	-0.0449	-0.0466	-0.0406	-0.0467

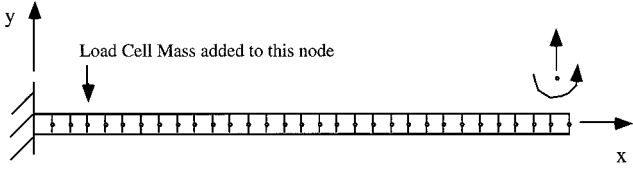


Fig. 1 Cantilevered beam discretized by a uniform mesh of 30 elements.

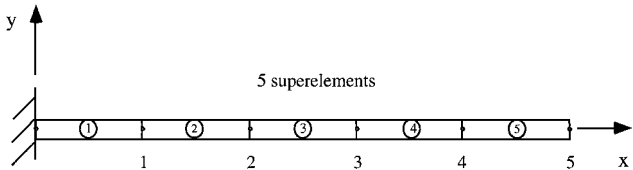


Fig. 2 Cantilevered beam showing the five 6-in.-long superelements.

study was securely clamped to an approximately 2000-lb monolith structure. The uniform rectangular cross section of the beam had a width of 0.0381 m (1.5 in.), a thickness of 0.00635 m (0.25 in.), and a length of 0.7620 m (30 in.). Hence, the cross-sectional area and inertia are  $2.4191 \times 10^{-4} \text{ m}^2$  and  $8.1279 \times 10^{-10} \text{ m}^4$ , respectively. The total mass is 0.531 kg with a calculated mean density of  $2757.09 \text{ kg/m}^3$ .

The beam was excited with a voice-coil actuator, where a load cell (mass of 0.01624 kg and attached 3 in. to the left of the clamping mechanism) measured the applied transverse force transmitted to the beam during testing. There were 22  $Y$  axis translational acceleration time-history data measured at 5 equidistant locations (6-in. intervals) along the beam with a piezoelectric accelerometer (mass of 0.00086 kg). These data were processed into frequencies and mode shapes using the eigensystem realization algorithm (ERA) method. The arbitrarily chosen limited number of measurement locations were used to represent an actual test where information on the structure is available at certain locations because, in general practice, limited numbers of sensors exist on a structure to gather data. To handle the degree-of-freedom mismatch between the analytic model and experiment, the present formulation utilized the system equivalent reduction expansion process (SEREP) reduction scheme to reduce the size of the FE model (FEM) matrices to that of the test degrees of freedom. The initial FEM consisted of 30 beam elements, shown in Fig. 1, whose global mass and stiffness matrices were reduced to the five translational test degrees of freedom using the SEREP reduction. Hence, the reduced global finite element mass and stiffness matrices were of size  $(5 \times 5)$ . Figure 2 shows the reduced FEM with the five superelements and five sensor locations.

Modal data processed from the experiment led to an approximate mean modulus of elasticity  $E$  for the beam of 68.5 GPa. To verify this mean modulus of elasticity, two scenarios were investigated (cases A and B). The first case underpredicted  $E$  by 5% (case A) for an initial value of 65.075 GPa, and the second case overpredicted  $E$  by 5% (case B) for an initial value of 71.925 GPa. All other parameters were kept the same. The mean SRFs from Eq. (2) and from the Monte Carlo simulation are listed in Table 1 for cases A and B. Note that, for case A, all SRFs are positive, indicating that the flexural rigidity needs to be increased by approximately 5%, and good agreement exists between Eq. (2) and the 22 experimental Monte Carlo simulations. Likewise, case B shows all negative SRFs, indicating that the flexural rigidity needs to be decreased by approximately 5%, and good agreement also exists between Eq. (2) and the 22

Table 2 SRFs obtained from the Monte Carlo simulation using case A FEM

Data	Beam superelement SRFs				
	$\alpha_1$	$\alpha_2$	$\alpha_3$	$\alpha_4$	$\alpha_5$
Mean	0.0600	0.0557	0.0538	0.0604	0.0536
Standard deviation	0.0092	0.0064	0.0053	0.0043	0.0109
COV, %	15.32	11.49	9.78	7.05	20.28

Table 3 SRFs obtained from the Monte Carlo simulation using case B FEM

Data	Beam superelement SRFs				
	$\alpha_1$	$\alpha_2$	$\alpha_3$	$\alpha_4$	$\alpha_5$
Mean	-0.0410	-0.0449	-0.0466	-0.0406	-0.0467
Standard deviation	0.0083	0.0058	0.0048	0.0039	0.0098
COV, %	20.29	12.90	10.22	9.50	21.06

Table 4 Estimated updated stiffness distributions for the model update/refinement problem for cases A and B

Type	Beam superelement distribution parameters, $\text{N}\cdot\text{m}^2$				
	$EI_1$	$EI_2$	$EI_3$	$EI_4$	$EI_5$
Case A					
Mean initial best-guess FEM	52.8925	52.8925	52.8925	52.8925	52.8925
Monte Carlo simulation	56.0651	55.8380	55.7374	56.0895	55.7284
Eq. (2)	56.3436	54.9324	55.0634	55.6678	54.6193
Standard deviation	0.4307	1.9946	0.3234	1.2775	0.8245
COV, %	0.76	3.63	0.59	2.29	1.51
Case B					
Mean initial best-guess FEM	58.4602	58.4602	58.4602	58.4602	58.4602
Monte Carlo simulation	56.0651	55.8380	55.7374	56.0895	55.7284
Eq. (2)	56.3436	54.9324	55.0634	55.6678	54.6193
Standard deviation	0.4300	2.0219	0.3270	1.2980	0.8354
COV, %	0.76	3.68	0.59	2.33	1.53

Monte Carlo simulations. Tables 2 and 3 list the SRF statistics, that is, standard deviations from the Monte Carlo simulation for cases A and B, respectively.

The correlation coefficient matrix for case A is

$$[\rho_{\text{SRF}}] = \begin{bmatrix} 1 & 0.1087 & 0.4400 & -0.3072 & -0.5413 \\ 0.1087 & 1 & -0.0318 & -0.5175 & -0.2855 \\ 0.4400 & -0.0318 & 1 & -0.0763 & -0.4104 \\ -0.3072 & -0.5175 & -0.0763 & 1 & 0.6023 \\ -0.5413 & -0.2855 & -0.4104 & 0.6023 & 1 \end{bmatrix}$$

The correlation coefficient matrix for case B is

$$[\rho_{\text{SRF}}] = \begin{bmatrix} 1 & 0.1087 & 0.4400 & -0.3072 & -0.5413 \\ 0.1087 & 1 & -0.0318 & -0.5175 & -0.2855 \\ 0.4400 & -0.0318 & 1 & -0.0763 & -0.4104 \\ -0.3072 & -0.5175 & -0.0763 & 1 & 0.6023 \\ -0.5413 & -0.2855 & -0.4104 & 0.6023 & 1 \end{bmatrix}$$

Finally, Table 4 lists the statistical data for the estimated model updated stiffnesses for cases A and B. It is shown that both cases produce similar mean values, standard deviations, and coefficients of variation (COVs).

The correlation matrix for the beam's flexural rigidity EI for case A is

$$[\rho_{EI}] = \begin{bmatrix} 1 & -0.1361 & -0.4930 & 0.0316 & -0.1551 \\ -0.1361 & 1 & 0.8678 & -0.9931 & -0.9532 \\ -0.4930 & 0.8678 & 1 & -0.8331 & -0.7422 \\ 0.0316 & -0.9931 & -0.8331 & 1 & 0.9768 \\ -0.1551 & -0.9532 & -0.7422 & 0.9768 & 1 \end{bmatrix}$$

The correlation matrix for the beam's flexural rigidity EI for case B is

$$[\rho_{EI}] = \begin{bmatrix} 1 & -0.1311 & -0.4844 & 0.0283 & -0.1559 \\ -0.1311 & 1 & 0.8712 & -0.9933 & -0.9545 \\ -0.4844 & 0.8712 & 1 & -0.8376 & -0.7489 \\ 0.0283 & -0.9933 & -0.8376 & 1 & 0.9774 \\ -0.1559 & -0.9545 & -0.7489 & 0.9774 & 1 \end{bmatrix}$$

The present method has been shown to solve successfully the probabilistic model update/refinement problem using experimentally measured modal data on a cantilever aluminum beam.

### Conclusions

A method has been presented to improve the robustness characteristics of current FEM updating methodologies by introducing the concept of probability theory. Measured statistical changes in natural frequencies and mode shapes, along with an initial analytic deterministic FEM are used to assess the integrity of the original model. Only the stiffness matrix was updated during the procedure and the mass matrix was assumed unchanged. The structural parameters of the system were modeled as correlated normal random variables. Stochastic expressions for SRFs were obtained that led to determination of estimated updated stiffness statistics. The method was applied using experimental data from a cantilever aluminum beam. The method was successfully able to adjust the stiffness parameters of an initial best-guess deterministic FEM to correct it using statistical data of experimentally measured modal properties. Two test cases were investigated where the initial model under-predicted (65.075 GPa) and over-predicted (71.925 GPa) the actual mean modulus of elasticity by 5.0%. For both scenarios, the method aptly corrected the under- and over-predictions. Overall, the method was successful in probabilistically updating the stiffness matrix of the experimental beam data.

### Acknowledgments

The authors would like to thank the National Science Foundation Dynamics Systems and Controls Program for the support of this work through a Presidential Faculty Fellows Program Award managed by Dev Garg.

### References

- <sup>1</sup>Berman, A., "Mass Matrix Correction Using an Incomplete Set of Measured Modes," *AIAA Journal*, Vol. 17, No. 10, 1979, pp. 1147, 1148.
- <sup>2</sup>Chen, J. C., and Garba, J. A., "Analytical Model Improvement Using Modal Test Results," *AIAA Journal*, Vol. 18, No. 6, 1980, pp. 684–690.
- <sup>3</sup>Imregun, M., and Visser, W. J., "A Review of Model Updating Techniques," *Shock and Vibration Digest*, Vol. 23, No. 1, 1991, pp. 9–20.
- <sup>4</sup>Mottershead, J. E., and Friswell, M. I., "Model Updating in Structural Dynamics: A Survey," *Journal of Sound and Vibration*, Vol. 167, No. 2, 1993, pp. 347–375.
- <sup>5</sup>Papadopoulos, L., and Garcia, E., "The Application of Probability Theory to Model Updating," *Proceedings of DETC'97: 1997 ASME Design Engineering Technical Conferences*, American Society of Mechanical Engineers, New York, 1997, pp. 1–11.
- <sup>6</sup>Papadopoulos, L., and Garcia, E., "Probabilistic Formulation of the Damage Detection Problem," *Proceedings of the 37th AIAA/ASME/ASCE/AHS Structures, Structural Dynamics, and Materials Conference*, AIAA, Reston, VA, 1996, pp. 2626–2634.
- <sup>7</sup>Papadopoulos, L., and Garcia, E., "Structural Damage Identification: A Probabilistic Approach," *AIAA Journal*, Vol. 36, No. 11, 1998, pp. 2137–2145.

A. Berman  
Associate Editor

## Shear-Sensitive Liquid Crystal Coating Method Applied Through Transparent Test Surfaces

Daniel C. Reda\* and Michael C. Wilder†  
NASA Ames Research Center,  
Moffett Field, California 94035-1000

### I. Introduction

THE objective of the present experiment was to explore application of the shear-sensitive liquid crystal coating (SSLCC) flow-visualization method through a transparent test surface. In this previously untested back-light/back-view mode, the exposed surface of the SSLCC was subjected to aerodynamic shear stress while the contact surface between the SSLCC and the solid, transparent surface was illuminated and viewed through the transparent surface. Figure 1a shows schematically the geometrical arrangement utilized in the conventional top-light/top-view mode,<sup>1–3</sup> and the new back-light/back-view mode is shown in Fig. 1b.

The optical properties of the liquid crystal molecular arrangement are reviewed in Refs. 4–6. Shear-sensitive cholesteric (chiral nematic) liquid crystal coatings are composed of helical aggregates of long, planar molecules arranged in layers parallel to the coated surface. Each layer of molecules is rotated, relative to the layer above and below it, about an axis perpendicular to the coated surface. The longitudinal dimension along the helical axis (the pitch) is on the order of the wavelengths of visible light. This layered, helical structure causes such materials to be extremely optically active. White light

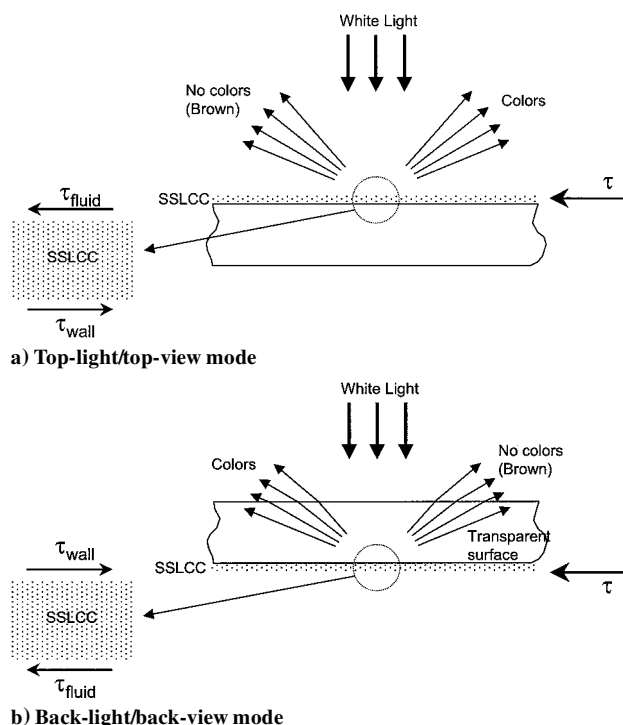


Fig. 1 Two SSLCC operational modes and the macroscopic view of the forces applied to the coating.

Received 10 February 2000; revision received 21 August 2000; accepted for publication 4 September 2000. Copyright © 2000 by the American Institute of Aeronautics and Astronautics, Inc. No copyright is asserted in the United States under Title 17, U.S. Code. The U.S. Government has a royalty-free license to exercise all rights under the copyright claimed herein for Governmental purposes. All other rights are reserved by the copyright owner.

\*Senior Staff Scientist, Space Technology Division. Fellow AIAA.

†Senior Research Scientist, ELORET. Member AIAA.